DETECTION OF METEORS IN SKY SURVEY IMAGE DATABASES

Dino Bekteševi[1], *Aleksandar Cikota*[2*], *Darko Jevremović*[3], *Dejan Vinković*[1,4†]

[1)]Physics Department, University of Split, Croatia,
[2)]Institute for Astro- and Particle Physics, University of Innsbruck, Austria,
[3)]Astronomical Observatory, Belgrade, Serbia;
[4)]Science and Society Synergy Institute, Croatia

ABSTRACT

Large angular size on the sky and random appearance make meteors difficult to explore by high-resolution high-sensitivity imaging detectors. The emergence of wide-field survey telescopes opened a possibility for exploring meteors with big telescopes utilizing sensitive imaging detectors and high quality photometric fluxes. Such telescopes have a long enough time coverage of a significant fraction of the sky to collect a relevant sample of low-brightness meteors. A large data throughput of these detectors requires a fast automatic detection of meteors on astronomical images. We discuss some issues related to meteor investigation using sky survey telescopes - detection rate of meteors from meteor showers, distinction between meteor and satellites trails, and algorithmic difficulties in automatic detection of meteors. We use the existing SDSS imaging database for developing automatic tools for meteor detection.

Index Terms— Meteors, SDSS, LSST, line detection, sky survey

1. INTRODUCTION

Meteors are transient optical phenomena caused by hypervelocity impacts of interplanetary dust (meteoroids) with the Earth's atmosphere. Meteoroids originate from asteroids and comets, and in rare cases from planets (e.g. Mars) or planetary satellites (e.g. Moon). Meteors are an interesting multidisciplinary research target due to their connection with a variety of physical processes - influence on the chemical and physical properties of the atmosphere, possible transport of prebiotic organic matter and its survival during hypervelocity flight, physics of extreme ablation under different atmospheric densities, composition of the meteoroid material originating from asteroids and comets, etc [1]. The theory of meteors has to address a wide range of hypervelocity physics - from individual molecular flow in a low density partially ionized atmosphere above ∼120 km altitude to fluid flow in a denser atmosphere below ∼90 km. The observations have to struggle with a large angular size of meteors on the sky combined with an unpredictable time of appearance. This typically makes telescope observations marginally suitable for meteor observations, while big telescope facilities, with a small field of view (FoV), almost completely ignore this type of observations.

The situation has changed with the emergence of wide-field robotic sky surveys, such as[1] the Sloan Digital Sky Survey (SDSS), the Pan-STARRS project, and the future Large Synoptic Sky Survey (LSST). Their sky coverage is big enough to intercept a significant number of meteors. Additionally, their high sensitivity of detectors provides access to the low brightness end of the meteor size distribution[3], while high-resolution imaging detectors can resolve the size of glowing meteor plasma and microstructure in their light curves.

2. PREDICTED NUMBER OF DETECTED METEORS

The advantage of telescopic meteor observations is the ability to detect low brightness meteors[2], which contributes to the knowledge on size distribution of meteoroids. For a given meteor stream, where meteoroids belong to the same parent source, we define [4] the mass index s as $dN(m) \propto m^{-s}dm$ where $dN(m)$ is the number of particles between m and $m+dm$. A similar relationship can be derived for meteor brightness, where we define the population index r. Two indexes are related as $s = 1 + 2.5 \log r$. If we use the canonical model of meteor flight through the atmosphere then we can derive the probability of meteor detection for given telescope properties. The canonical model consists of a set of equations [1] describing the change in the meteor velocity v, its mass m, altitude h and brightness M (in magnitudes). In Figure 1 we show an example of the predicted number of meteors per hour per FoV of SDSS telescope (FoV=3° and estimated 10^m limiting magnitude) for a meteor shower similar to Per-

*The author performed the work while at the University of Split, Croatia
†Corresponding author: dejan@iszd.hr

[1]http://www.sdss.org; http://pan-starrs.ifa.hawaii.edu; http://lsst.org
[2]http://www.imo.net/tele/science

doi: 10.2788/1823

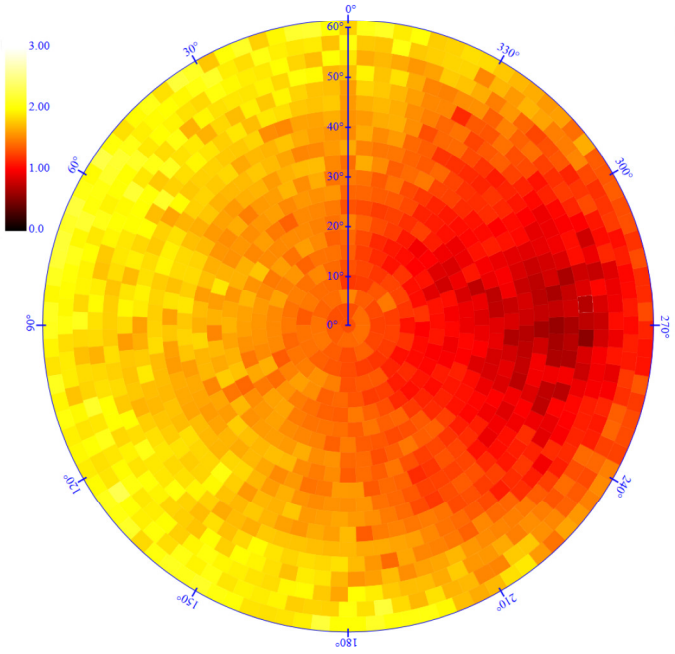

Fig. 1. The zenith view of the probability of detecting meteors similar to Perseids with the SDSS telescope during one hour of observations under visual Zenithal Hourly Rate of 100. The colors scale show the number of meteors per hour per field of view. The maximum zenith angle of telescope tilt is 60°. This example is for a meteor entry angle (radiant zenith angle) fixed to $z = 45°$, an initial meteor speed of 59 km/s, a mass index of $s = 2.07$ ($r = 2.86$), a meteoroid density of 0.75 g/cm^3, the minimum meteoroid mass of 16 μg (the minimum size 115 μm), an ablation coefficient of σ=0.1 s^2/km^2, and a shape-density coefficient of K=1.46 cm^2/g$^{2/3}$ [5].

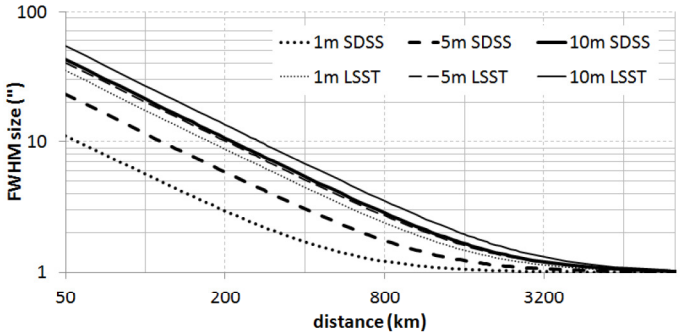

Fig. 2. Angular size of defocused images of meteor glowing plasma spheres at different distances from SDSS (thick lines) and LSST (thin lines) telescopes and three meteor sizes (1m, 5m and 10m). Dependance of the image size on the object distance can be used to differentiate between meteors and satellites.

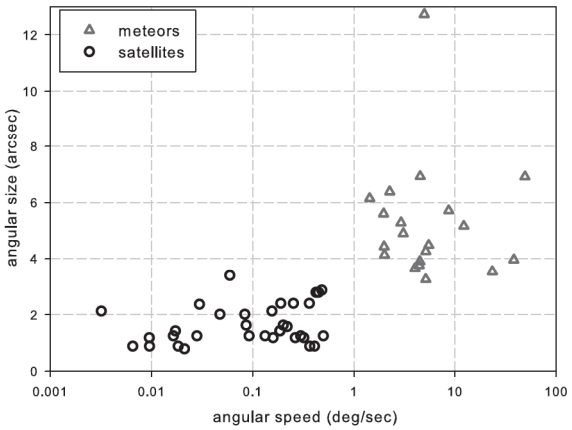

Fig. 3. Angular size of defocused images of satellites and meteors compared with their angular speed on SDSS images. Data collected by Tomislav Čizmić Marović.

seids with 100 meteors per hour activity. We used a Monte Carlo method for calculating a large number of randomly distributed meteors all over the sky.

It is interesting that when we visually inspected the SDSS image database for meteors during highly active meteor showers, we did not find as many meteors as expected. Considering a strong dependence of meteor number on the mass (population) index, we can conclude that the mass distribution of low brightness meteors does not follow the distribution typically observed in bright (visual) meteors. This type of statistical analysis can be implemented into the automatic meteor detection programs for future sky survey telescopes.

3. METEOR SIZE AND SATELLITES

Large diameter telescopes are ideal for resolving the physical size of meteor plasma sphere. The size σ_m of a defocused image of a meteor plasma at distance d and with diameter D is $\sigma_m^2 = (D^2 + D_m^2)/d^2 + \sigma_{atm}^2$, where D_m is the telescope mirror diameter and σ_{atm} is the atmospheric seeing. Meteor plasma spheres are expected to be at least meters in size, which has been explored by telescopic observations [3], radar observations and theoretical modeling [6].

Figure 2 shows the size of meteor images with SDSS and LSST telescopes, with 1arcsec atmospheric seeing. The meteors are highly resolved, with about 10arcsec in size, as they appear at distances less than 200 km. Notice that images of satellites have less than about 2arcsec in angular size, which makes satellite trails clearly distinctive from meteor trails. Moreover, satellites show a very smooth, often periodically variable, light curves, unlike meteors that have irregular brightness (flickering during flight). In SDSS we can also derive angular speed of moving objects thanks to the drift-scan imaging method. In drift-scan, each row in an

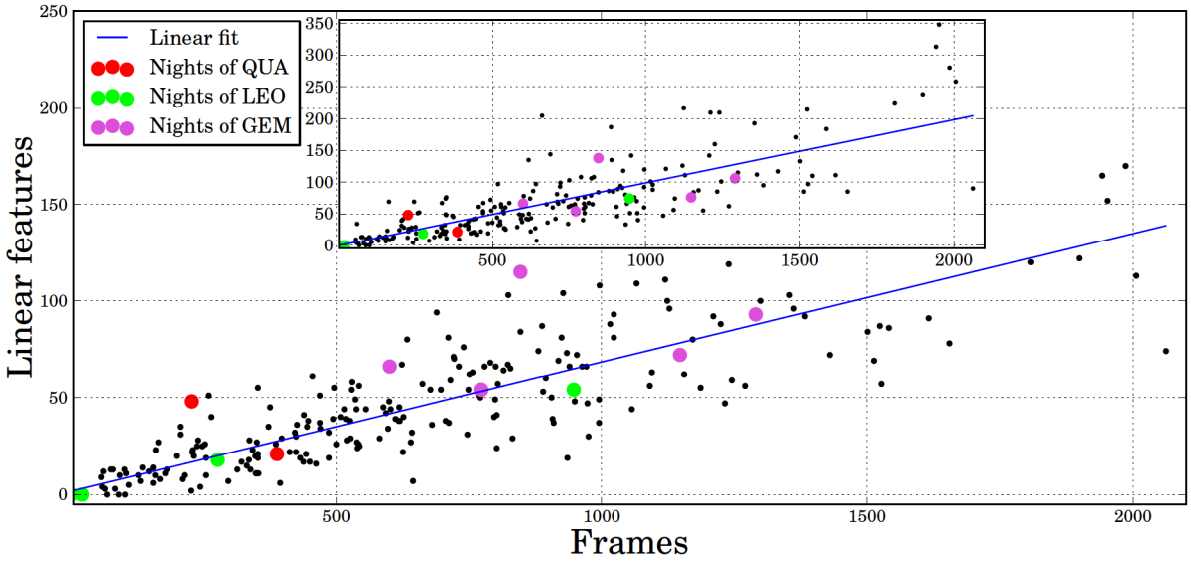

Fig. 4. The current status of our method for linear feature detection - each point is a cumulative number of frames in SDSS (r and i filters) for a given day in all years combined together (horizontal axis) and the number of detected linear features in these frames (vertical axis). The smaller graph shows all detected lines, while the big plot shows data after the removal of obvious satellites by hand. The result is still probably dominated by satellites, but we work on automatic detection of meteors by measuring the angular width of the lines (see Figures 2 and 3). Days when we expect meteors from some meteor showers (the maximum activity ± 2 days) are marked in color: QUA = Quadrantids, LEO = Leonids, GEM = Geminids.

image has its own time of readout. Hence, the row where a line starts corresponds to the moment when an object entered the FoV, while the row where this line ends corresponds to the exit time. This gives an exact angular speed on the flying object. Since meteors appear as very fast objects, while satellites have a slower angular speed, this method can be used as an independent method for separating meteor lines from satellites on images. This is demonstrated in Figure 3 on a small sample of handpicked data. Meteors and satellites were recognized by their appearance (ligthcurve properties, connection with the known meteor radiants) and then their angular size and speed were measured. The clustering of meteors above a well defined angular size confirms that the angular size of linear features on images can be used as a method for separating meteors from satellites even when the angular speed is unavailable (e.g. in LSST images).

4. AUTOMATIC DETECTION OF METEORS

We are developing a numerical method for automatic detection of meteors on high-resolution astronomical images. The algorithms are tested on SDSS image database, but they will be adjusted for the upcoming Pan-STARRS data release and the future LSST imaging data stream. Typically lines can be detected using Hough transform, but we encountered problems with a large fraction of false positives if stars are not properly removed. Hence, we devised one algorithm that removes a large fraction of stars and noise in the images, such that dominantly meteor signal remains. In this case the meteor is detected with the RANSAC method [2]. The other algorithm uses the list of identified objects in the analyzed images by the SDSS Photo pipeline. These objects are then removed from the image, followed by image noise reduction and compression of brightness dynamical scale. Canny [7] edge detection is performed on such prepared images, which allows fitting of minimum area rectangles to all Canny edges that form a closed loop. This enables detection of a linear feature. However, to find its exact position, the standard Hough [8] method is applied on the image, which results in detection of a line.

We currently test the robustness and execution speed of these algorithms on the SDSS image database. We work mostly on SDSS's r and i filters, but when the algorithm becomes optimized we will search through the entire SDSS database. The current execution times of the algorithm on single SDSS images is less than one second per frame. This includes 0.1-0.3 seconds for star removal and 0.15-0.2 seconds for detection of bright trails or 0.3-0.6 seconds for detection of dim trails. Figure 4 shows the current number of detected lines, where our main concern is how to avoid false positives and false negatives. The next step will be implementation of an algorithm that will fit the line bright-

Fig. 5. An example of a meteor in SDSS images. Based on the association with known meteor shower radiants, we identified this meteor as a Northern Taurid. The images were taken on November 18, 2001. The left image is in r filter and it shows the moment of meteor entering the FoV (TAI=04:57:21.42) and the right image is in g filter with the moment of meteor exiting the FoV (TAI=04:56:27.77). Times are reversed because TAI attached to the image rows show the time of readout. Hence, the difference between TAIs of meteor entrance and exit includes the image exposure time plus the time of flight of the meteor through the FoV. Based on these values and the measured length of the meteor trail ($1.638°$) we derived the angular speed of $6.63°/s$. Meteors typically appear between 110km and 90km altitude, which gives us a possible distance to the meteor. Based on the angular width of the trail along the path, its angular speed and the known speed of Northern Taurids, and defocusing trends in Figure 2, we calculated the possible size of glowing meteor plasma to be between 4.7m and 6.2m. Notice how defocusing increased along the meteor path as the meteor moves closer to the telescope.

ness profile to a theoretical double-peaked image profile of a moving defocused object.

Once we build a database of meteor images, we can search for their possible association with the known meteor showers. In Figure 5 we show an example of a Northern Taurid. Based on the reconstructed geometry of its flight, we estimate the size of its meteor plasma to be in meters. More detailed information can be extracted when we start investigating brightness of such meteors visible in different SDSS filters and other properties of the lightcurves. The final product will be a fast automated process of meteor detection that can be executed in real time as the images arrive from a survey telescope.

5. REFERENCES

[1] Ceplecha, Z. et al. 1998, "Meteor Phenomena and Bodies", Space Science Reviews, 84, 327

[2] Fischler, M.A. & Bolles, R.C. 1981, "Random Sample Consensus: A Paradigm for Model Fitting with Applications to Image Analysis and Automated Cartography", Comm. of the ACM, 24, 381-395

[3] Iye, M. et al. 2007, "SuprimeCam Observation of Sporadic Meteors during Perseids 2004", Publications of the Astronomical Society of Japan, 59, 841

[4] Verbeeck, C. & Ryabova, G.O. 2011, "Calculation of the incident flux density of meteors by numerical integration: Improved geometrical approach", Journal of Atmospheric and Solar-Terrestrial Physics, 73, 901

[5] Ceplecha, Z., & McCrosky, R. E. 1976, Journal of Geophysical Research, 81, 6257

[6] Dyrud, L. et al. 2008, "Plasma and Electromagnetic Simulations of Meteor Head Echo Radar Reflections", Earth Moon and Planets, 102, 383

[7] Canny, A. 1986, "Computational Approach to Edge Detection", IEEE Trans. on Pattern Analysis and Machine Intelligence, 8, 679

[8] Hough, P.V.C. 1959, "Machine Analysis of Bubble Chamber Pictures", Proc.Int. Conf. High Energy Accelerators and Instrumentation